Composite Structures 159 (2017) 81–95

Contents lists available at ScienceDirect

Composite Structures

journal homepage: www.elsevier.com/locate/compstruct

Strengthening of metallic beams with different types of pre-stressed un-bonded retrofit systems

F. Kianmofrad [a], E. Ghafoori [b,*], M.M. Elyasi [c], M. Motavalli [a,b], M. Rahimian [a]

[a] University of Tehran, School of Civil Engineering, Tehran, Iran
[b] Empa, Swiss Federal Laboratories for Materials Science and Technology, Structural Engineering Research Laboratory, Dübendorf, Switzerland
[c] Sharif University of Technology, School of Mechanical Engineering, Tehran, Iran

ARTICLE INFO

Article history:
Received 25 April 2016
Revised 11 August 2016
Accepted 12 September 2016
Available online 20 September 2016

Keywords:
CFRP laminates
Aluminum beams
Steel beams
Bridges
Strengthening
Flexibility method
Pre-stressed CFRP tendon

ABSTRACT

Unlike bonded retrofit systems, un-bonded systems do not need any surface preparation prior to bond application, which reduces the overall time and cost of a retrofit plan. Because the carbon fiber reinforced polymer (CFRP) plate in the un-bonded (tendon) systems is not bonded to a metallic substrate, different variants of the retrofit systems can be developed to ease application in the field. This paper presents four different variants of the prestressed un-bonded retrofit (PUR) systems: trapezoidal PUR (TPUR), triangular PUR (TriPUR), Flat PUR (FPUR), and Contact PUR (CPUR) systems. Analytical solutions based on the flexibility approach are developed to predict the behavior of the metallic beams retrofitted with the PUR systems. A finite element (FE) model is created to simulate the behavior of the retrofitted beams. The results of the analytical solutions are compared with those obtained from the FE model. The results from the analytical and numerical models have been compared with the results of an experimental study on steel and aluminum beams retrofitted with the PUR systems. A series of parametric studies are performed to investigate the influence of different parameters such as the type of the PUR system and the CFRP pre-stress level on the behavior of the retrofitted beams. The results show that for a specific CFRP pre-stress level, all four different PUR systems result in approximately the same stress reduction in the steel beam bottom flanges. Therefore, it is possible to use any of the four pre-stressing technique depending on the requirements of the structure to be pre-stressed.

1. Introduction

Over the last few decades, bridges have experienced a massive increase in static and dynamic loads because of developments in transportation technology worldwide [1–4]. While trains and vehicles have become heavier and faster, roads and bridges have become older and their ability to withstand the increased volume of traffic loads has decreased. Because the reconstruction of deficient bridges is expensive and time-consuming, bridge authorities often consider a retrofit option.

1.1. Retrofit with pre-stressed carbon fiber reinforced polymer (CFRP) plates

The usage of FRP materials instead of steel plates or tendons is a new procedure for retrofitting purposes and their pre-stress technics are essentially different. The conventional methods for retrofitting usually utilize bulky steel plates, which are heavy, difficult to install and are prone to corrosion and fatigue of their own. Compared to the CFRP material, steel plates are heavy, and their installation process often requires crane. Furthermore, using heavy steel strands can increase the deadweight of the bridge, which is not good for fatigue, as the mean stress level is increased and it results in higher fatigue failure risks [5,6]. Since the 1990s, CFRP materials have gained much attention for retrofitting and construction purposes [7]. The CFRP material has a high strength-to-weight ratio, high corrosion resistance and excellent fatigue performance [8]. Metallic members have traditionally been strengthened using non-pre-stressed CFRP plates. However, in non-pre-stressed retrofit systems, the dead loads are not transferred to the CFRP plates and only a portion of the live load is transferred to the CFRP plates. As an alternative, by using pre-stressed CFRP plates, a portion of the dead load is transferred to the CFRP plates in addition to the live load [9,10]. The fatigue life of steel members has been substantially increased by using bonded CFRP plates [11–18]. It has been shown that pre-stressed CFRP laminate is capable of preventing fatigue crack initiation in steel members [5,19,20]. Furthermore,

* Corresponding author.
E-mail address: elyas.ghafoori@empa.ch (E. Ghafoori).

http://dx.doi.org/10.1016/j.compstruct.2016.09.020
0263-8223/

Nomenclature

CFRP	carbon fiber reinforced polymer
PUR	pre-stressed un-bonded retrofit
TPUR	trapezoidal PUR
TriPUR	triangular PUR
FPUR	flat PUR
CPUR	contact PUR
PBR	pre-stressed bonded reinforcement
FE	finite element
DOF	degree of freedom
e_p^i	initial deflection of CFRP plate(s)
e	deviator height (eccentricity of CFRP plate from beam)
$\theta_A,\ \theta_B,\ \theta_C$	slope of the beam at A, B and C cross sections, respectively
φ	complementary angle of the angle between deviator and CFRP plate
$\delta_B,\ \delta_C$	deflection of the beam at B and C cross sections, respectively
L_b	beam length
L_e	effective beam length between C and C'
L	length of the CFRP plate after system deformation
L_i	initial length of the CFRP plate
L_0^i	initial length of the CFRP plate before pre-stressing (in FPUR and CPUR systems)
Δ	change or elongation in the initial length of the CFRP plate:$\Delta = L - L_i$
l	loading distance from the deviator point (i.e., node C)
$\delta_{BC}^F,\ \delta_{BC}^T$	vertical displacement of node B relative to node C because of the external force F and tensile force of CFRP plate T, respectively
δ_i	vertical displacement at node i
δ_{ji}	relative vertical displacement between i and j nodes
δ_M	beam mid-span deflection
σ_p^U	tensile strength of the CFRP material
$E_p,\ E_s$	Young's modulus of the CFRP plate and steel beam, respectively
$A_p,\ A_s$	cross-sectional areas of the CFRP plate and steel beam, respectively
I	moment of inertia of the beam cross-section
G_s	transverse shear modulus of steel
F	external vertical load applied by an actuator
T	tensile force in the CFRP plate
K	shear coefficient (equal to 0 or 1)
PSL	pre-stress level (in percentage)
$\sigma_P,\ \varepsilon_P$	stress and strain in the CFRP plate
$\sigma_b^u,\ \varepsilon_b^u$	stress and strain in beam upper flange
$\sigma_b^l,$	stress and strain in beam lower flange
$\delta_{BC}^F,\ \delta_{BC}^T$	vertical displacement at node B relative to node C because of the external force F and tensile force at CFRP plate T, respectively
δ_i	vertical displacement at node i
δ_{ji}	relative vertical displacement between i and j nodes
δ_M	beam mid-span deflection

Ghafoori et al. [21,22] have shown that it is possible to arrest fatigue crack growth (FCG) in metallic members using pre-stressed CFRP plates. CFRP materials have good long-term behavior. It has superior fatigue behavior, much better than steel, and they have high corrosion resistance.

1.2. Bonded vs. un-bonded retrofit system

The majority of the existing research on CFRP strengthening of metallic members has used CFRP material bonded to the steel substrate. The efficiency of the bonded retrofit system is mainly dependent on the behavior of the CFRP-to-steel bond joint. Sophisticated surface preparation is required prior to bonding the CFRP to the steel member to maximize the efficiency of the composite system and reduce the risk of debonding. Many studies have raised concerns about the influence of environmental conditions (e.g., elevated or subzero temperatures, water and moisture and ultraviolet light) and dynamic loads (e.g., fatigue, impacts and earthquakes) on the behavior of the CFRP-to-steel bond joint (e.g., [18,23,24]).

Because of these concerns, which are mainly associated with the long-term performance of the CFRP-to-steel bond joints, Ghafoori and Motavalli [25–27] have designed and tested a pre-stressed un-bonded retrofit (PUR) system. In contrast to the bonded system, the un-bonded system works without using any bond; instead, it uses a pair of friction clamps to connect the CFRP plates to the steel member.

1.3. Advantages of the PUR systems

The developed un-bonded system has advantages over the traditional bonded systems that are briefly mentioned in the following. The PUR system offers a fast installation procedure because there is no need for extensive surface preparation prior to the bond application. It has been shown that the required amount of time to prepare the metallic beams that were retrofitted with the bonded retrofit system was nearly twice that required for the preparation of beams that used the un-bonded retrofit system [25]. The un-bonded retrofit system can be used for strengthening of metallic members with rough (e.g., because of corrosion) or obstructed (e.g., because of rivet heads) surfaces. In particular, the proposed retrofit system is suitable for retrofitting of cultural structures, where no additional element is allowed to be attached or bonded permanently to the original members. In contrast to CFRP bonded systems, the elements of the un-bonded retrofit systems can be easily detached from the original structures.

The un-bonded retrofit systems need mechanical clamps to connect the CFRP plates to the steel member. The clamps are constructed from steel that is compatible with the steel member to be retrofitted. The concerns related to corrosion of the steel clamps are irrelevant because the system is used for retrofitting of a steel structure. Bridge authorities usually apply anti-corrosion coatings and paints to bridge members every few years. Similar measures can be taken to protect the clamps against corrosion.

1.4. Different variations of the PUR systems

In the bonded retrofit systems, CFRP plates are always attached to the steel member using a type of adhesive bond. Unlike bonded retrofit systems, un-bonded retrofit systems offer different varieties of retrofit configurations. A trapezoidal PUR (TPUR) system has already been developed and tested [27]. The system was used for fatigue strengthening of riveted girders in a 120-year-old railway metallic bridge in Switzerland [28]. In this paper, analytical and numerical models are developed to estimate the behavior of the TPUR system. The results from modeling are then compared

with existing experimental results on steel and aluminum beams retrofitted with the PUR systems.

The TPUR system is not applicable for all different structures, for instance, for the case when there is not enough space beneath the bridge to attach the system. Because the system is un-bonded, it is possible to design different variants of the retrofit system. In this paper, three new PUR systems, namely Triangular PUR (TriPUR), Flat PUR system (FPUR) and Contact PUR (CPUR), are presented. Analytical models are developed to predict the linear-elastic behavior of the systems. A critical comparison between the behavior of the PUR systems (i.e., TPUR, TriPUR, FPUR and CPUR systems) is performed. The aim of this paper is to compare the performance of different PUR systems. The results provide a better understanding of the behavior of different PUR systems and will help engineers choose the retrofit solution that eases the field retrofit application based on the geometrical limitations of the steel element to be retrofitted. Performing numerous experiments to investigate the effects of each key factor (i.e., beam dimensions or material, CFRP cross-section, pre-stress level, retrofitting system, loading point, etc.) is difficult, therefore, in this study, a series of analytical solutions was proposed to make this comparison easier.

2. Pre-stressing technique and assumptions

A schematic view of the TPUR system developed by Ghafoori and Motavalli [27] is shown in Fig. 1, as well as different parameters. Furthermore, Fig. 2(a) and (b) depicts a schematic view of the system before and after the pre-stressing. The two ends of the CFRP plates are fixed inside a pair of friction clamps that transfer the force from the CFRP plates to the metallic beam. The CFRP plate without any tension is gripped inside the mechanical clamps but initially has an eccentricity, e^i, as shown in Fig. 2(a). As the eccentricity, e, between the CFRP plate and the steel substrate is increased (using a deviator with adjustable height), the CFRP pre-stress level increases, and a negative bending moment is applied to the beam, as shown in Fig. 2(b). The height of the deviator is increased until the desired level of CFRP pre-stress is reached. Note that while pre-stressing, there is no vertical load on the beam. After strengthening, vertical loads are applied to the top flange of the metallic I-beam. As the vertical load increases, the upward deflection in the beam decreases, and for the larger value of vertical loads, the beam deflects downward (see Figs. 2 and 3). The advantages of the proposed retrofit system are i) there is no need to bond the CFRP to the metal, ii) installation is fast because there is no need for surface preparation, iii) there are no traffic interruptions for bond curing, iv) there is no damage to the existing metallic beam (e.g., no need for holes, grinding and gluing), v) pre-stressing is easy, vi) the CFRP pre-stress level can be increased/decreased easily by adjusting the height of deviator and vii) if necessary, the retrofit system can be uninstalled without any residual damage to the original steel member. Details about the design of different components of the TPUR system, including the friction clamps and the deviators, can be found in [27,28]. The pre-stressing technique presented in this paper for the TPUR system is manual, however, the same method can be implemented using hydraulic jacks.

It is assumed that CFRP laminates are only loaded axially and that their bending stiffness is negligible. A linear elastic material behavior is considered for all elements. It is also assumed that the clamps and the deviators are rigid and do not deform. The friction between the saddle and the CFRP plate is assumed to be negligible. Note that although the materials are considered linear elastic and the deformation of the beam is small, there is a large geometric deformation in the CFRP plates caused by the change in length of the deviators (see C and C' in Fig. 2). Therefore, the system is geometrically non-linear and statically indeterminate.

3. Analytical solution for the TPUR system

In this section, an analytical solution based on the flexibility method [29,30] is presented. Explicit solutions that can be used to predict the behaviors of the retrofitted systems are derived. Because of the symmetry of the system, $A'B'$ and $B'C'$ sections need the same calculations as AB and BC, respectively. The axial force in the CFRP plates is T and is assumed to be constant along the CFRP length (friction at the saddle point is ignored). The beam has ten degrees of freedom (DOF), but because of the symmetry, they will be reduced to five DOF (θ_A, θ_B, θ_C, δ_B and δ_C). The CFRP plates have one longitudinal DOF (Δ). The TPUR system is statically indeterminate (one degree of indeterminacy). Therefore, to use the flexibility approach, the CFRP plates are assumed to be cut at the ends, which makes the beam statically determinate. As observed in Fig. 3, the deformations of the beam and the CFRP plate at the clamps are linked by a compatibility equation.

Note that the vertical loads, F, can be applied to any arbitrary points between B and B' on the top flange of the beam, as shown in Fig. 2(a). The distance between the deviator and the vertical load is l. When the vertical load is applied between the deviator and the mid-span, "l" has a positive value, while when the load is applied between the deviator and the clamp, "l" has a negative value (see Fig. 2(a)). The middle part of the beam (CC') behaves like a simply supported beam with two symmetric bending moments, M_C, applied at its ends (see Fig. 2). Because the beam behaves within the linear elastic domain, the principle of superposition can be used when the loading position is between C and the beam mid-span ($0 \leqslant l \leqslant \frac{L_e}{2}$). The rotation of point C can be found by the Conjugate-Beam Method [31] as

$$\theta_C = \begin{cases} \frac{M_C L_e}{2E_s I} & -b < l < 0 \\ \frac{M_C L_e}{2E_s I} + \frac{Fl}{2E_s I}(L_e - l) & 0 \leqslant l \leqslant \frac{L_e}{2} \end{cases} \quad (1)$$

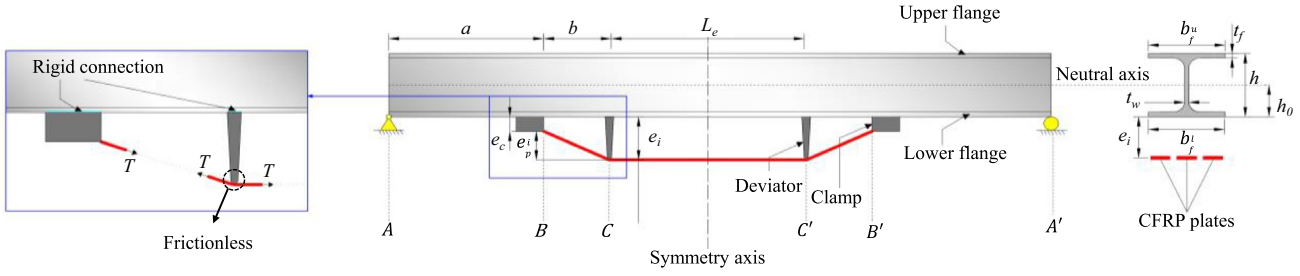

Fig. 1. Schematic view of a metallic I-beam retrofitted with the TPUR system.

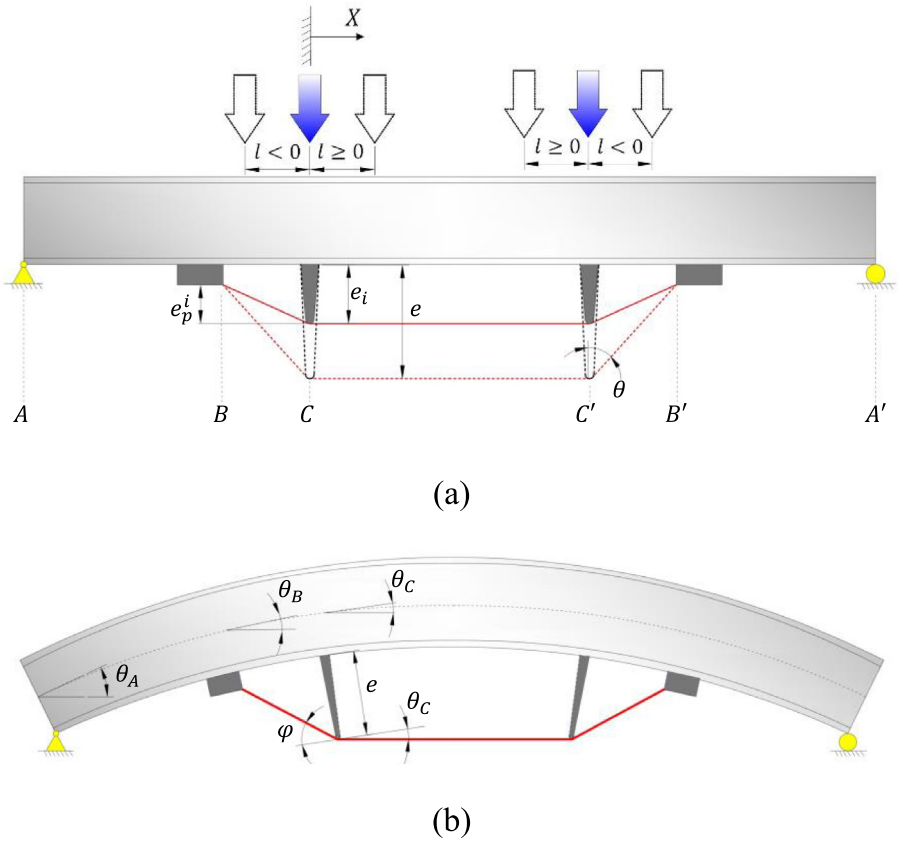

Fig. 2. (a) Vertical loads are either applied between C and the mid-span ($l \geqslant 0$) or between B and C ($l < 0$), (b) when the deviator height, e, increases, the CFRP pre-stress also increases, which applies a negative bending moment to the metallic beam.

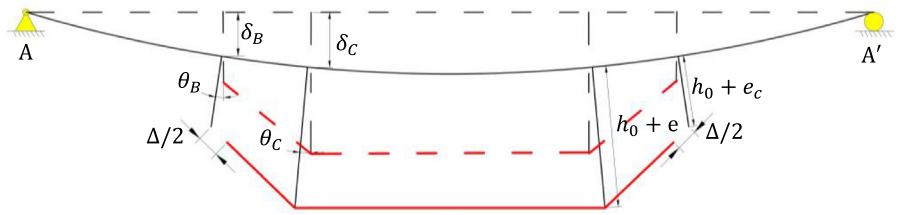

Fig. 3. To make the beam statically determinate, it is assumed that the CFRP plate is cut.

where F is the external vertical point load, E is the Young's modulus of elasticity of the metal, and the subscript s refers to steel. I is the moment of inertia of the beam cross-section and L_e is the length of part CC'. M_i and θ_i are the moment and the rotation at node i. Subscript i refers to the desired node along the beam (e.g., node B or C) and is positive counterclockwise. In this paper, angles are in radians. l is the loading position and is the distance from the deviator (node C), as shown in Fig. 2(a). M_C is considered to be the total moment at the node C and is given by

$$M_C = M_{Ce} + M_{Ci} \tag{2}$$

where M_{Ce} and M_{Ci} are the external and the internal bending moments at node C, respectively. Because the friction between the deviator and the CFRP plate (the friction at the saddle) is ignored, M_{Ce} and M_{Ci} are given by

$$M_{Ce} = -T(e + h_0)(\cos\theta_c - \cos\varphi) \tag{3}$$

and

$$M_{Ci} = \begin{cases} F(a+b) + Fl - T(b\sin\varphi + (e_c + h_0)\cos\varphi) & -b < l < 0 \\ F(a+b) - T(b\sin\varphi + (e_c + h_0)\cos\varphi) & 0 \leqslant l \leqslant \frac{L_e}{2} \end{cases} \tag{4}$$

where T is the tensile force in the CFRP plate(s). a and b are the distances between the support and the clamp and between the clamp and the deviator, respectively. h_0 is the vertical distance between the neutral axis of the beam and the bottom surface of the beam's bottom flange (see Fig. 1). φ is the complementary angle of the angle between the deviator and the CFRP plate(s), as shown in Fig. 2, and is defined as

$$\sin\varphi = \frac{e - e_c}{\sqrt{b^2 + (e - e_c)^2}} \tag{5}$$

$$\cos\varphi = \frac{b}{\sqrt{b^2 + (e - e_c)^2}} \tag{6}$$

where e_c is the thickness of the clamps. a is the length of part AB, and b is the length of part BC. e is the eccentricity between the CFRP plate and the beam's bottom flange (i.e., the deviator height). Substituting Eqs. (3) and (4) into Eq. (2) yields

$$M_C = \begin{cases} (a+b+l)F - T(b\sin\varphi + (e_c+h_0)\cos\varphi + (e+h_0)(\cos\theta_C - \cos\varphi)) & -b < l < 0 \\ (a+b)F - T(b\sin\varphi + (e_c+h_0)\cos\varphi + (e+h_0)(\cos\theta_C - \cos\varphi)) & 0 \leqslant l \leqslant \frac{L_e}{2} \end{cases} \tag{7}$$

Substituting Eq. (7) into Eq. (1) gives

$$\theta_C = \begin{cases} \frac{L_e}{2E_sI}[(a+b+l) - T(b\sin\varphi + (e_c+h_0)\cos\varphi + (e+h_0)(\cos\theta_C - \cos\varphi))] & -b < l < 0 \\ \frac{L_e}{2E_sI}[(a+b)F - T(b\sin\varphi + (e_c+h_0)\cos\varphi + (e+h_0)(\mathrm{Cos}\theta_C - \cos\varphi))] + \frac{Fl}{2E_sI}(L_e - l) & 0 \leqslant l \leqslant \frac{L_e}{2} \end{cases} \tag{8}$$

Considering part BC as a cantilever beam, the rotation of the beam at point B is given by

$$\theta_B = \begin{cases} \theta_C - \frac{T}{E_sI}\left(\frac{b^2}{2}\sin\varphi + b(e_c+h_0)\cos\varphi\right) + \frac{F}{E_sI}\left(\frac{b^2-l^2}{2} + ab\right) & -b < l < 0 \\ \theta_C - \frac{T}{E_sI}\left(\frac{b^2}{2}\sin\varphi + b(e_c+h_0)\cos\varphi\right) + \frac{F}{E_sI}\left(\frac{b^2}{2} + ab\right) & 0 \leqslant l \leqslant \frac{L_e}{2} \end{cases} \tag{9}$$

Note that in Eq. (9), θ_B and θ_C are expressed in terms of T. On the other hand, the axial deformation in the CFRP plates is

$$\Delta = \frac{TL_i}{E_pA_p} \tag{10}$$

Subscript p refers to the CFRP plates, and A_P is the total cross-sectional area of the CFRP plates. L_i is the initial length of the CFRP plate

$$L_i = L_e + 2\sqrt{b^2 + (e_i - e_c)^2} \tag{11}$$

The compatibility equation that involves geometrical characteristics of the system is

$$\Delta = L - L_i \tag{12}$$

where L is the final length of the CFRP plates and is written as (see Fig. 3)

$$L = L_e + 2\left[\sqrt{b^2 + (e_i - e_c)^2} + (e+h_0)\sin\theta_C + \frac{\theta_{BC}(e_c+h_0)}{\cos\varphi}\right] - \frac{T}{E_sA_s}(L_e + 2b) \tag{13}$$

In Eq. (13), the first term and the first term in the bracket are from Eq. (11) (i.e., the initial length of the CFRP plates). The other terms in the bracket refer to deformation because of the rotation of the cross sections at node C and B, respectively. The last term refers to deformation in the CFRP plate because of the axial deformation of the beam. e_i is the initial height of the deviator (i.e., the initial eccentricity between the CFRP plates and the beam's lower flange) at which the tension in the CFRP plates is equal to zero (i.e., $e_i = e_p^i + e_c$). Substituting Eqs. (11) and (13) into Eq. (12) yields

$$\Delta = 2\left(\sqrt{(e-e_c)^2 + b^2} - \sqrt{(e_i - e_c)^2 + b^2} + (e+h_0)\sin\theta_C + \frac{\theta_{BC}(e_c+h_0)}{\cos\varphi}\right) - \frac{T}{E_sA_s}(L_e + 2b) \tag{14}$$

where $\theta_{BC} = \theta_B - \theta_C$ and can be obtained from Eqs. (8) and (9). As the deformations are small in the beam, it can be assumed that

$$\sin\theta_C \approx \theta_C \tag{15}$$

and

$$\cos\theta_C \approx 1 \tag{16}$$

Considering the above simplifications, by substituting Eqs. (8) and (9) into Eq. (14) and then replacing the obtained expression for Δ into Eq. (10), T can be calculated as

$$T = \begin{cases} \frac{2\gamma_3A_s(Fb(2eL_e(a+b+l)+bh(\gamma_1+L_e)+2\gamma_1(be_c+ah)+hL_e(a+l)+4ae_c\gamma_1)-Fl^2\gamma_1(2e_c+h)+4E_sIb(\gamma_1-\gamma_2))}{b\gamma_3(4I(2b+L_e)+4A_s(be_c(e_c+e)+eL_e(e+h))+A_sh(2b(h+e)+(hL_e+6be_c)))+4b\gamma_4I(2\gamma_2+L_e)} & -b < l < 0 \\ \frac{2\gamma_3A_s(4E_sI(\gamma_1-\gamma_2)+F((2e+h)(l(L_e-l)+L_e(a+b))+\gamma_1(2a+b)(2e_c+h)))}{\gamma_3(4I(2b+L_e)+4A_s(be_c(e_c+e)+eL_e(e+h))+A_sh(2b(h+e)+(hL_e+6be_c)))+4\gamma_4I(2\gamma_2+L_e)} & 0 \leqslant l \leqslant \frac{L_e}{2} \end{cases} \tag{17}$$

where

$$\begin{aligned} \gamma_1 &= \sqrt{b^2 + (e-e_c)^2} \\ \gamma_2 &= \sqrt{b^2 + (e_i - e_c)^2} \\ \gamma_3 &= E_pA_p \\ \gamma_4 &= E_sA_s \end{aligned} \tag{18}$$

Here, h is the height of the I-beam (see Fig. 1) and $h = 2h_0$ (for symmetric cross-sections). After calculating T, the system becomes statically determinate and other parameters (e.g., mid-span deflection, δ_M, stresses and strains) can be calculated based on the method [31] presented in Appendix A.

4. Analytical solutions for the TriPUR, FPUR, and CPUR systems

As has been mentioned in Section 1.3, there are situations in which the TPUR system cannot be installed or is difficult to install on the bridge members. For instance, in some cases, there is not enough space under the bridge to place the deviators, or there might be concerns about the aesthetic aspects of the structure after retrofitting. In this section, three different configurations of the PUR system are presented, as shown in Fig. 4. Among the different presented PUR systems (i.e., TPUR, TriPUR, FPUR and CPUR) for strengthening of a bridge member, the one that best fits the geometrical limitations of the structure can be selected. The analytical solution for these PUR systems can be obtained by modifying the solution presented for the TPUR system in Section 3 and will be explained in this section.

4.1. The TriPUR system

The TriPUR system includes two clamps that fix the CFRP plate to the beam's bottom flange. The system includes a deviator with an adaptive length under the beam mid-span, as shown in Fig. 4 (a). The eccentricity, e, between the CFRP plate and steel beam can be adjusted by setting different heights for the deviator. The

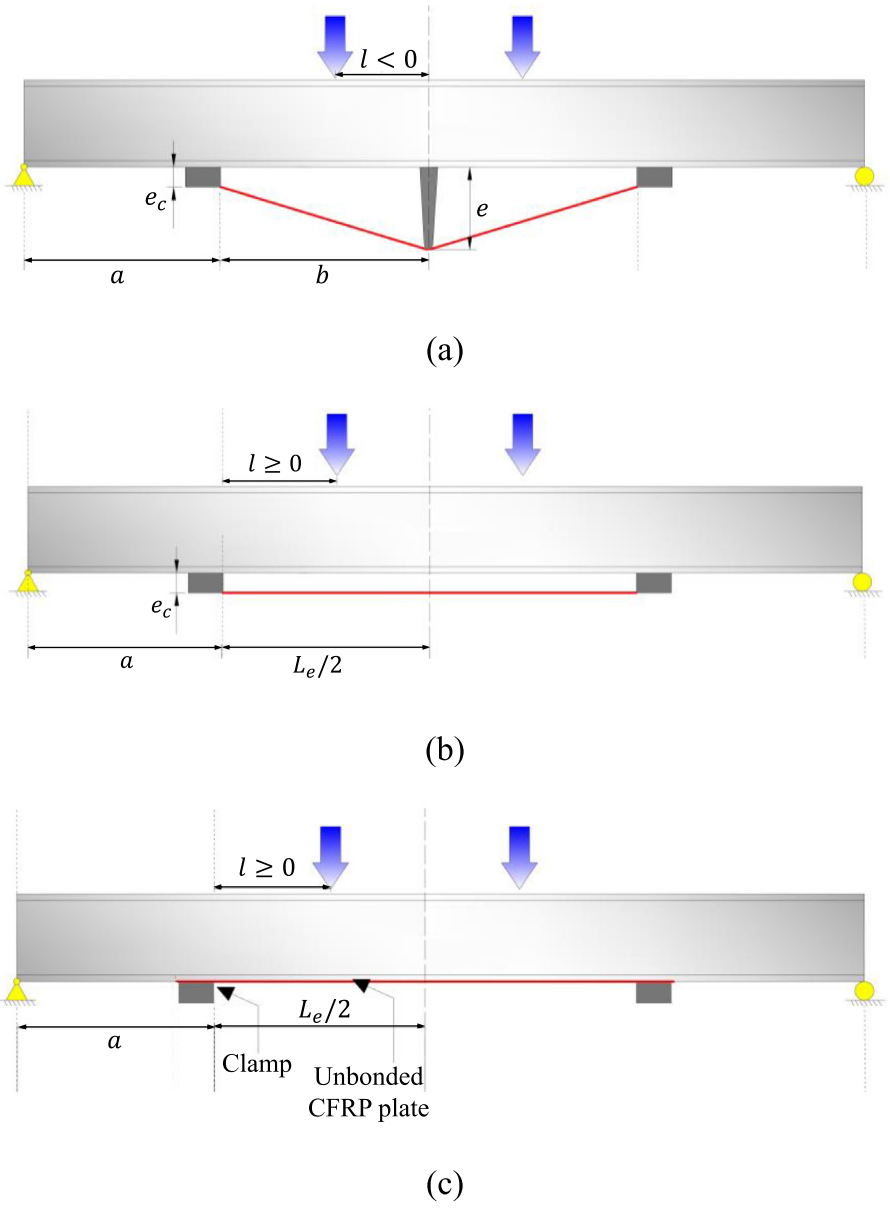

Fig. 4. Three other configurations of the PUR system: (a) the TriPUR system, (b) the FPUR system and (c) the CPUR system.

system works in the same way as the TPUR system; however, it has only one deviator. Note that it is possible to add this section to end of Section 3 (because of their similarities), but given the long length of Section 3, the description about the TriPUR system is given in this section. Accordingly, the analytical method developed for the TPUR system in Section 3 can be modified for the TriPUR system. The parameter L_e should be set to a small value (e.g., 10 mm), which implies that the deviators are at the same position and act like one deviator. Other parameters mentioned in Section 3 remain the same. Note that for the TriPUR system, it is always the case that $-b < l \leqslant 0$.

4.2. The FPUR system

In the FPUR system, the deviators in the TPUR system are removed (see Fig. 4(b)). A hydraulic jack can be used to pre-stress the CFRP plates from the right or the left end of the CFRP plate. Based on the method presented in Section 3, the parameter b should be set to a small value $b \cong 0$, which means that the deviator and the clamp are at the same position. This would result in $\theta_B \cong \theta_C$, and therefore, $\theta_{BC} \cong 0$. Furthermore, the deviator height has to be set equal to the thickness of the clamp, $e = e_i = e_c$, because node B and node C (see Fig. 2(a)) are in the same position. Hence, based on Eq. (11), L_i will become equal to L_e (i.e., $L_i \cong L_e$).

There are two approaches to pre-stressing the CFRP laminates in the FPUR and the CPUR systems. One method is to fix the left end of the CFRP plate to the steel beam using a clamp and pull the right end of the CFRP using an actuator that is fixed to the beam. Once the required CFRP pre-stress level is reached, the right end of the CFRP plate is fixed to the beam using a clamp. The second method is to pull the CFRP plate using an independent reaction frame, as shown in Fig. 5. In this method, the pre-stressing is applied by a hydraulic jack that is connected to the independent reaction frame. Upon achieving the desired CFRP pre-stress, the

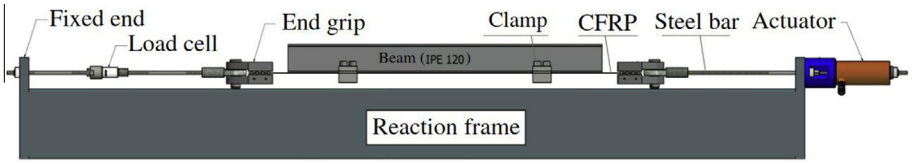

Fig. 5. Schematic of the details of the pre-stressing set-up with an independent reaction frame for pre-stressing CFRP laminates (mainly for laboratory uses) [25].

force in the CFRP plate is locked using two clamps. The latter pre-stressing technique is mainly suitable for laboratory applications, while the former is good for on-site pre-stressing of the CFRP laminates, because it does not need any reaction frame. More details about the first method of strengthening will be published in a future paper.

The analytical method in this paper assumes that the second pre-stressing technique (i.e., using an independent reaction frame) is used. Therefore, in the FPUR system, the pre-stressing is applied before attaching the CFRP plate to the beam flange, while in the TPUR system, the pre-stressing was applied after installation of CFRP plates (by using deviators). Hence, the meaning of L_i in the FPUR system is slightly different from that in the TPUR system. Here, L_i refers to the initial length of the CFRP plate after the pre-stressing and installation procedure (i.e., just before vertical loads are applied). After the pre-stressed CFRP is attached to the beam, the pre-stress level is decreased because of deformation of the beam. To calculate the reduced pre-stress level, it is assumed that the initial length of the CFRP plates before pulling (without any tension) is L_0^i and that after pre-stressing, it becomes L_i (i.e., $L_i \cong L_e$). Therefore, it is given by

$$L_0^i = L_i - \Delta_L \tag{19}$$

where Δ_L is the initial deformation of the CFRP plate because of pre-stressing with the actuator and is given by

$$\Delta_L = \sigma_p^U L_i \frac{PSL}{100E_p} \tag{20}$$

σ_p^U is the ultimate tensile strength of the CFRP plate and PSL is the percentage of the "pre-stress level" in the CFRP plate. By considering Eq. (13), Eq. (14) can be rewritten as

$$\Delta = L - L_0^i = L_e + 2(e_c + h_0)\theta_C - \frac{T}{E_s A_s}(L_e) - L_0^i \tag{21}$$

Because $0 \leqslant l < \frac{L_e}{2}$, Eq. (17) can also be rewritten to calculate T (in the FPUR system):

$$T = \frac{E_P A_P}{L_0^i}\Delta = \frac{100\gamma_1^2 A_s F(h_0 + e_c)(l(L_e - l) + aL_e) + \gamma_1\gamma_2 I \cdot A_p \cdot L_e \cdot PSL \cdot \sigma_p^U}{100\gamma_1^2(IL_e + A_s L_e(e_c^2 + h_0^2 + 2e_c h_0)) + \gamma_2 IL_e(100\gamma_1 - A_p \cdot PSL \cdot \sigma_p^U)} \tag{22}$$

where

$$\gamma_1 = E_p A_p \qquad \gamma_2 = E_s A_s \tag{23}$$

Other parameters have been determined similar to the methodology described in Section 3 and Appendix A.

4.3. The CPUR system

The CFRP plate in the CPUR system has direct contact with the bottom flange of the beam. The system is implemented by removing the deviators and placing the CFRP plates between the clamp and the beam lower flange, as shown in Fig. 4(c). The two pre-stressing methods that have been explained in Section 4.2 for the FPUR system can also be used for the CPUR system. Note that the analytical formulations for the CPUR system are developed for strengthening using an independent reaction frame (see Fig. 5). It is assumed that the curvature of the lower flange surface can be approximated by three straight lines, BC, CC' and $C'B'$, as shown in Fig. 6. The proposed method in Section 3 can be used for this system by setting the height of the deviator (i.e., e and e_i) and the thickness of the clamps all to a unique small value (e.g., $e = e_i = e_c = 1$ mm). It is also considered that $L_i = L_e + 2b$. Therefore, to obtain the final CFRP pre-stress level (after pre-stressing loss), a similar procedure to that described in Section 4.2 is followed here:

$$\Delta = L - L_0^i = L_e + 2(b + (e_c + h_0)\sin\theta_C) + \frac{\theta_{BC}(e_c + h_0)}{\cos\varphi} - \frac{T}{E_s A_s}(L_e + 2b) - L_0^i b \tag{24}$$

$$T = \frac{E_P A_P}{L_0^i}\Delta \tag{25}$$

Here, Eq. (24) is used to rewrite Eq. (17) (instead of Eq. (17)) for $e = e_i = e_c$. Substituting Eq. (24) into Eq. (25) gives T (for the CPUR system). Other parameters and equations can be obtained by the same procedure as described in Section 3 and Appendix A.

5. FE modeling

FE modeling of an I-beam that has been strengthened with the TPUR system is explained in this section. The FE model helps to provide a better understanding about the state of stress distribution along the steel beam after retrofitting, for example, see Fig. 7. Note that in Fig. 7, the tension in the CFRP plate is much bigger than the tension in the beam flanges. Therefore, in order to see the stress distribution in the beam clearly, the upper limit of the stress is restricted to 450 MPa, which is the reason why stress in

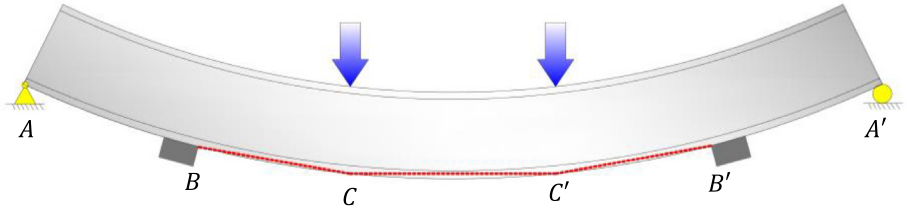

Fig. 6. It is assumed that the CFRP plate in the CPUR system has three straight segments.

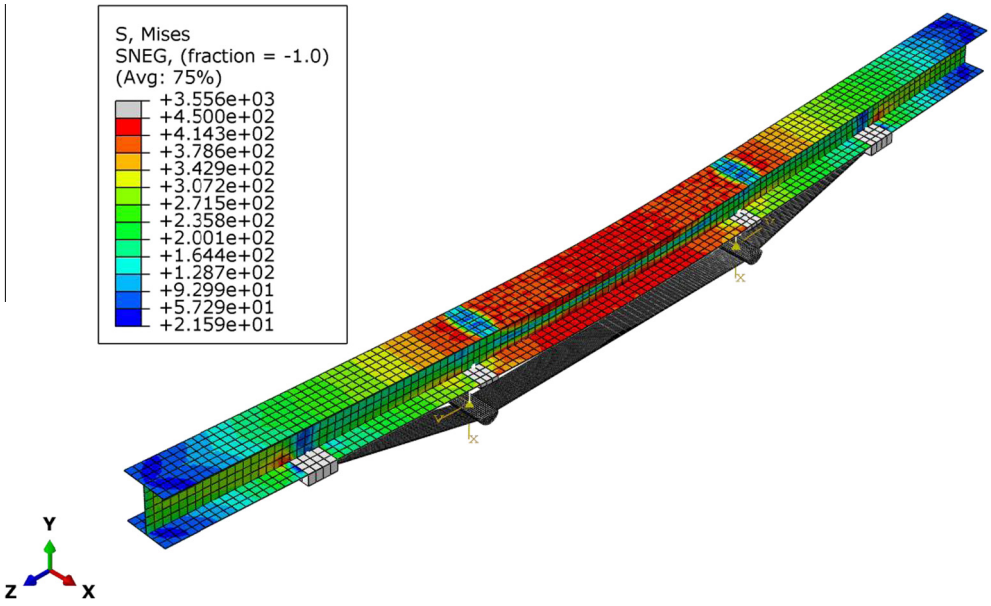

Fig. 7. The stress distribution (in MPa) along the beam can be predicted using the FE model.

Table 1
Geometrical properties for the two test sets A and B (dimensions are in mm).

Test-Set	Beam	Section	Lb*	a	b	Le	l	h	b_f^u	b_f^l	t_w	t_f	e_c	e_p^i	$e_i = e_p^i + e_c$
First Set	A	IPBl240	5000	825	825	1700	0	230	240	230	7.5	12	55	104	159
Second Set	B	IPE120	1200	220	180	400	0	120	65	65	4.4	6.2	1	0	1

* L_b is the length of the beam.

Table 2
Type of PUR system and the CFRP pre-stressing level used for the First Set and the Second Set.

First Set			Second Set		
Sample	System	Pre-stress	Sample	System	Pre-stress
AR	–	Unstrengthened	BR	–	Unstrengthened
AT0	TPUR	0%	BC0	CPUR	0%
AT15	TPUR	15%	BC20	CPUR	20%
AT30	TPUR	30%	BC40	CPUR	40%

Table 3
Mechanical and geometrical properties of the CFRP and the steel used for the First Set and the Second Set.

Test-Set	σ_p^U (Mpa)	E_p (GPa)	E_s (GPa)	A_p (mm^2)	A_s (mm^2)
First Set	2450	158.5	209	180	7350
Second Set	2800	165	199.3	70	1350

the CFRP plates is shown in gray. All geometrical and material properties are identical to those from the experiment performed by Ghafoori and Motavalli [27]. This information is briefly summarized as the 'First Set' in Tables 1–3. All materials were assumed to have linear-elastic behavior. Eight-node shell elements with reduced integration (S8R) were used to mesh the beam (with a general mesh size of 40 mm). The boundary conditions of the model simulate the actual support condition of a simply supported beam, as shown in Fig. 8. Rigid body constraints were used at the ends of the beam to prevent stress concentration at the supports. Different parts of the retrofit system are connected with different constraints, as illustrated in Fig. 8. Four-node discrete rigid elements (R3D4) were used to mesh the clamp and the deviator parts (i.e., the base and the saddle) at a general mesh size of 40 mm. The base and the saddle are connected to each other using a translator connector (see Fig. 9). Furthermore, the clamp and the deviator bases were connected to the lower flange using a "tie constraint". Four-node shell elements with reduced integration (S4R) were used to mesh the CFRP plate. The mesh size was not uniform and was reduced from 40 mm at the clamp location to 5 mm at the contact area where the CFRP plate is in direct contact with the saddle (see Fig. 9). The contact between the CFRP plate and the saddle is assumed to be frictionless. The simulation consisted of the two static steps of CFRP pre-stressing and loading. The first step simulates the pre-stressing procedure. In this step, the length of the deviators between the base and the saddle is increased, and there-

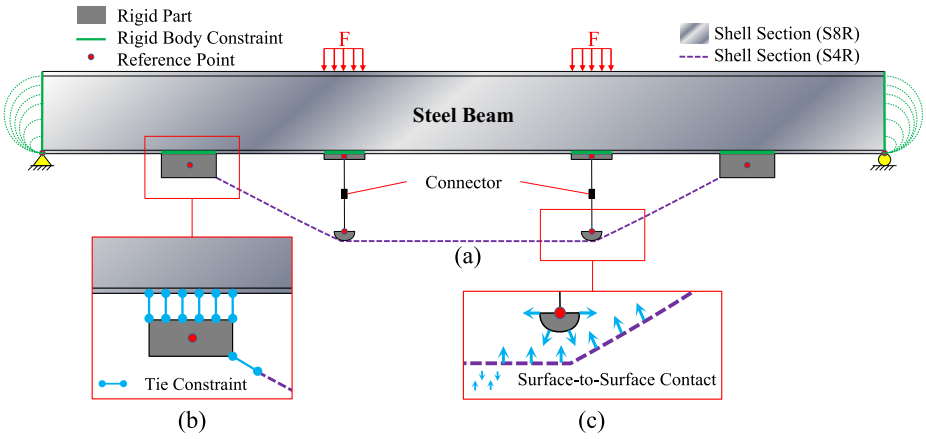

Fig. 8. (a) Constraints between different parts of the TPUR system. (b) Rigid parts (i.e., clamps and deviators) are tied to the lower flange, and also clamps are tied to the end of the CFRP plate. (c) A frictionless contact between the saddle and the CFRP plate is defined.

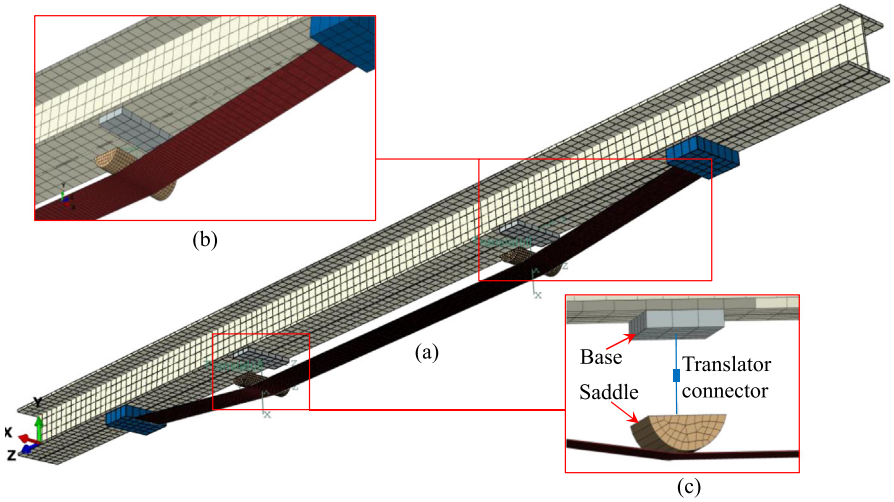

Fig. 9. (a) The beam retrofitted with the TPUR system. (b) Mesh size in the CFRP plate becomes finer near the saddle. (c) Parts of the deviator (i.e., the base and the saddle) are connected using a translator connector.

fore, the CFRP plate is pre-stressed. In the second step, the external vertical loads are applied to the upper flange of the steel beam.

6. Numerical and experimental verifications

In this section, the qualitative results of the analytical method developed are presented and compared with the numerical and experimental results.

6.1. Numerical verifications

Fig. 10 shows the pre-stress level in the CFRP plate as the length of the deviator increases. In the absence of external vertical loads, as the height of the deviator, *e*, increases, the stress in the CFRP plate increases. Ghafoori and Motavalli [27] developed a method for predicting the pre-stress level as a function of the eccentricity, e. Their method is based on the assumption that the beam is rigid, and therefore, it has negligible upward deformation when subjected to a negative bending moment. Fig. 10 compares the CFRP pre-stress level obtained from the so-called "rigid beam" assumption with the results of the presented analytical and numerical method. From Fig. 10(a), it is seen that the numerical and analytical solutions show good agreement, while the rigid-beam assumption overestimates the CFRP pre-stress level. As observed in Fig. 10 (a) and (b), both the pre-stress level and the mid-span deflection have a nonlinear relation to the deviator height. Fig. 11 shows the strain in the CFRP plate and the beam flanges as a function of the deviator height for Beam A, which is retrofitted using the TPUR system as described in Tables 1–3.

6.2. Experimental verifications with aluminum and steel I-beams

Zhu et al. [32] have performed a series of static tests to study the flexural behavior of aluminum I-beams retrofitted using pre-stressed CFRP tendons. The FPUR, the TriPUR, and the FPUR systems, each with different pre-stress levels, have been used for strengthening of the beams. Aluminum 6061-T6 with a Young's modulus of 70 GPa and a yield strength of 236 MPa was used. The retrofitted aluminum beams have been tested in a four-point loading set-up. Further details about the material and geometrical properties of the tests can be found in [32]. Fig. 12(a) shows the load deflection behavior of the aluminum I-beams retrofitted with the TriPUR and the FPUR systems with 40 kN and 80 kN pre-stress levels, respectively. Fig. 12(b) demonstrates the strains at the bot-

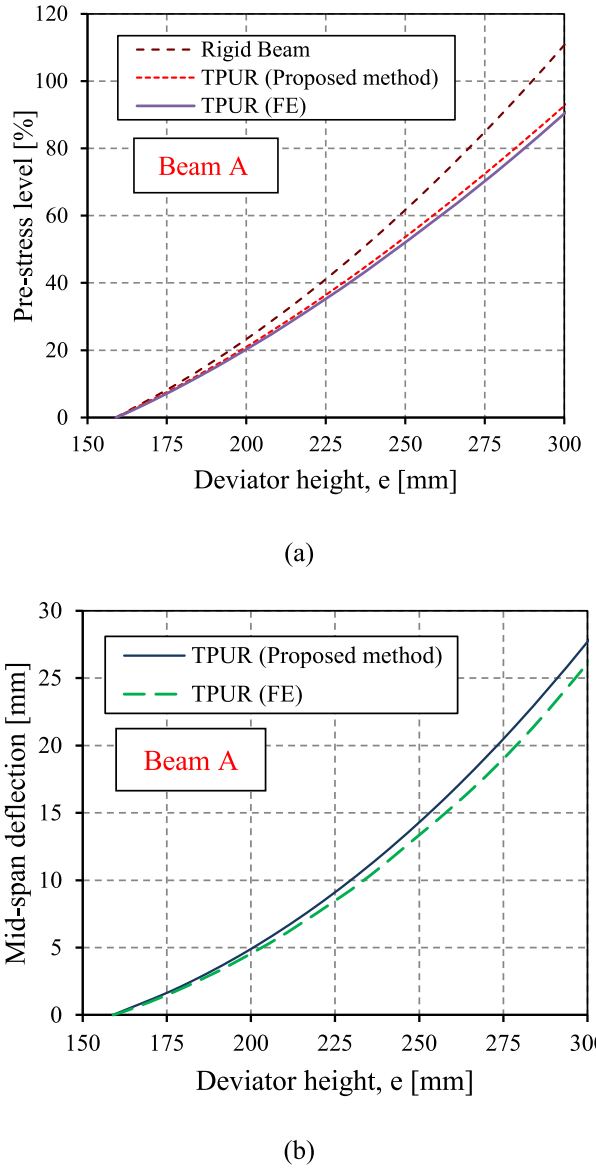

Fig. 10. (a) The CFRP pre-stress as a function of the deviator height for the I-beam strengthened with the TPUR systems (for e_i = 159 mm and F = 0 kN). (b) The mid-span upward deflection as a function of the deviator height (for e_i = 159 mm and F = 0 kN).

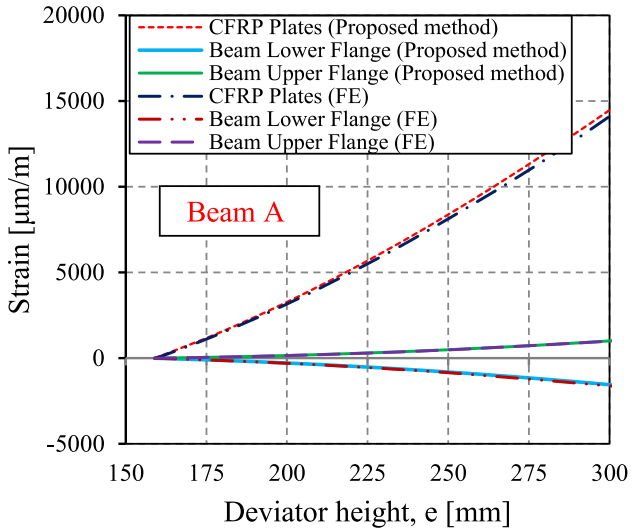

Fig. 11. The strains on the CFRP plates and the beam upper and lower flanges as a function of the deviator height for the TPUR system (for e_i = 159 mm and F = 0 kN).

tom and the upper flanges of the aluminum beams when the external vertical load increases from 0 kN to 35 kN. The results of experiments are compared with those obtained from the proposed analytical solutions and show good agreement between theory and practice.

Ghafoori et al. [19,25] have studied the behavior of steel I-beams retrofitted with the TPUR and the CPUR systems. The tests were performed in a four-point load set-up. Details about the geometrical and material properties can be found in Tables 1–3. Although, the focus of [24] is on the 'lateral torsional buckling', their experimental results in the linear-elastic domain (before the buckling) are useful for the current research to provide a good understanding of the elastic flexural behavior of the retrofitted girders. Fig. 13(a) shows the load-deflection behavior of the steel I-beams retrofitted by the TPUR system with different CFRP pre-stress levels of 0.0%, 15%, and 30% (see Table 2). The vertical loads are applied to the upper flange at the cross-section where the deviators are located (i.e., l = 0). The results of the experimental, numerical and the proposed analytical models are shown in Fig. 13(a). It is seen from this figure that as long as the system behaves in the elastic domain, there is a negligible difference between the results of the analytical, the numerical and the experimental methods. It is also seen that the stiffness of the retrofitted beams slightly increases as the pre-stress level increases. The reason for this increase in the stiffness is because the eccentricity, e, between the CFRP plate and the steel beam is larger for beams retrofitted by high pre-stress levels. Therefore, as the eccentricity increases, the moment of inertia of the beam cross-section increases, and therefore, the stiffness increases.

Similar to Fig. 13(a) and (b) shows the load-deflection behavior of Beam B (see Table 1) retrofitted with the CPUR system (see Table 2) with different pre-stress levels of 0% (specimen BC0), 20% (specimen BC20) and 40% (specimen BC40). The results of the experimental, numerical and analytical methods show good agreement in the elastic domain. The retrofitted specimens show only 6% more stiffness than the reference unstrengthened specimen (i.e., BR). However, the load-deflection curves for different CFRP pre-stress levels remain almost parallel to each another in the elastic domain. The latter shows that the magnitude of the CFRP pre-stress level does not have any effect on the stiffness of the retrofitted specimens, provided that the eccentricity, e, between the CFRP plate and the beam remains constant. From Fig. 13(b), it can be observed that as the pre-stress level increases, the negative bending moment increases, and therefore, a larger initial upward deflection at the beam mid-span is observed.

Fig. 14 shows the strain in the CFRP plates, the lower flange and the upper flange at the mid-span of specimen AT30, which has been strengthened with the TPUR system with CFRP pre-stress level of 30%. Fig. 15 shows the strain in the CFRP plate, the lower flange and the upper flange of the specimens retrofitted with the CPUR system. Different pre-stress levels of 0% (specimen BC0 shown in Fig. 15(a)), 20% (specimen BC20 shown in Fig. 15(b)) and 40% (specimen BC40 shown in Fig. 15(c)) were used for strengthening. It can be seen that the results of the experiments show good agreement with those obtained from numerical and analytical simulations. Based on Fig. 15, the difference between the experimental and analytical results is less than 1% in the CFRP plate and 3% in the steel beam flanges.

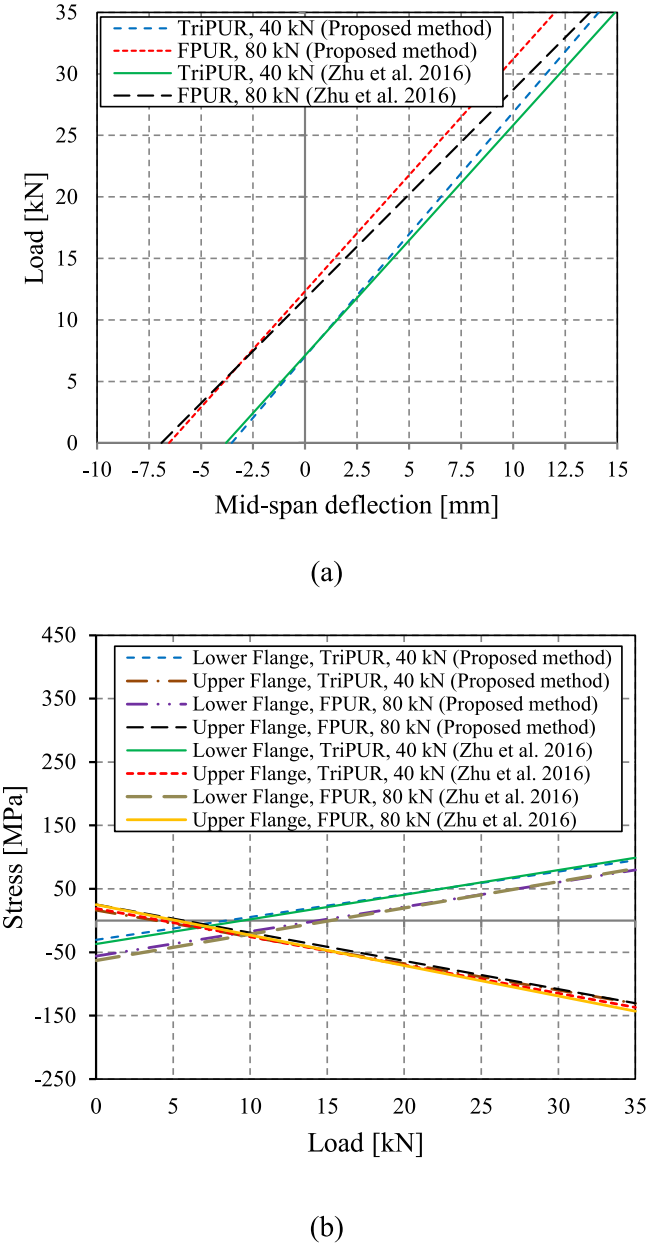

Fig. 12. (a) The load deflection behavior of the aluminum beams strengthened by the TriPUR and the FPUR systems with 40 kN and 80 kN pre-stress levels, respectively. (b) The strains at the bottom and the upper flanges of the aluminum beams when the vertical load increases.

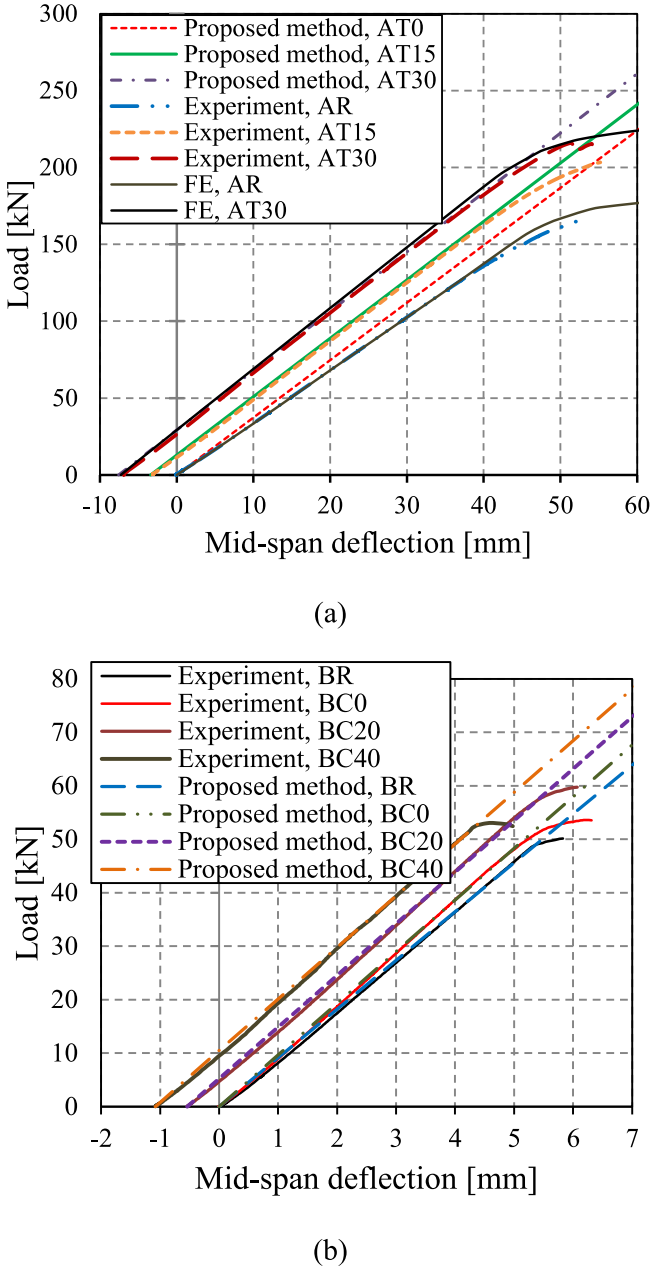

Fig. 13. Comparison between the load–deflection behaviors of the unstrengthened beam with the beams strengthened by (a) the TPUR system with the CFRP pre-stress level of 0% (specimen AT0), 15% (specimen AT15) and 30% (specimen AT30), (b) the CPUR system with the CFRP pre-stress level of 0% (specimen BC0), 20% (specimen BC20) and 40% (specimen BC40).

7. Parametric study

In this section, a parametric study is performed to examine the efficiency of different configurations of the PUR system. The effects of different parameters such as the CFRP pre-stress level and the position and magnitude of the applied vertical loads on the flexural behavior of the retrofitted beams are investigated. Furthermore, the influence of the location of the deviators along the beam and the geometric and mechanical properties of the CFRP plates on the strain distribution along the beam is discussed.

7.1. Effect of loading position

In the previous examples of strengthening using the TPUR system, the vertical loads were applied at the beam cross-section that includes the deviators. Fig. 16 shows the effect of the position of the vertical loads between the clamp and the beam mid-span. All parameters that are used in analytical modeling are given in Tables 1 and 2 (see Beam A and the First Set); however, the loading position l is different. Fig. 16(a) shows the strain in the CFRP plate as a function of the position of the vertical load for a beam retrofitted with the TPUR system. The results are given for three different pre-stress levels of 0% (specimen AT0), 15% (specimen AT15) and 30% (specimen AT30) with two different vertical loads of 50 kN and 130 kN. From Fig. 16(a), as the load position approaches the beam mid-span, the strain in the CFRP plate increases.

The strains in the lower and upper flanges of the beam are shown in Fig. 16(b) and (c), respectively. As the loading position

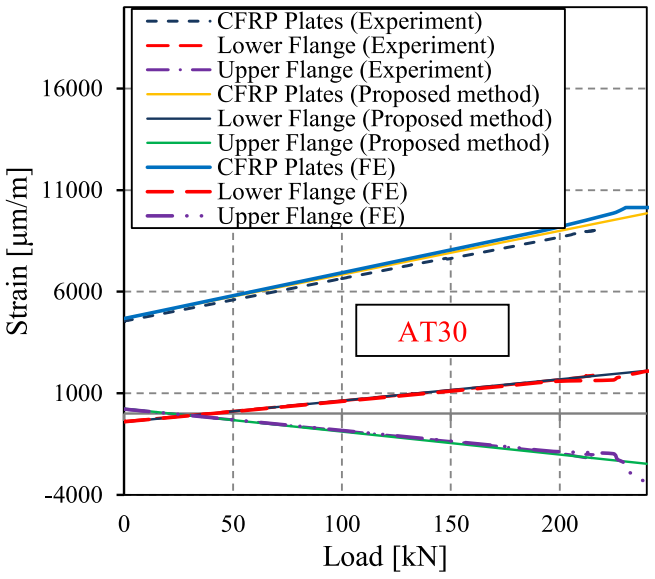

Fig. 14. The strains on the CFRP plate and the beam upper and lower flanges for specimen AT30 (strengthened by the TPUR system with 30% CFRP pre-stress).

approaches the beam mid-span, the magnitude of the strains in the lower and the upper flanges of the retrofitted beam increases. Fig. 16(d) shows the mid-span deflections of the beam retrofitted with different CFRP pre-stress levels of 0%, 15% and 30% subjected to vertical loads of 50 kN and 130 kN. The maximum deflections are achieved when the loads are applied at the beam mid-span.

7.2. Efficiency of different retrofit systems

In this subsection, the effect of retrofitting the beams by using different PUR systems is discussed. Geometrical details of Beam A (see Table 1) are used here. The CFRP pre-stress level and the load position are identical for the different beams. Table 4 shows the dimensions that were adopted for all of the PUR systems. In the TriPUR system, it is assumed that $e_p^i = 50$ mm. All of the PUR systems have a pre-stress level of 30%.

Fig. 17 shows the load-deflection behavior of the beam retrofitted with different PUR systems. From this figure, it can be seen that the TPUR and TriPUR systems show slightly larger stiffness compared to the other retrofit systems. Furthermore, the beams retrofitted by the TPUR system have the maximum magnitude of the initial upward deflection.

Fig. 18 depicts the strain in the CFRP plate, the lower flange and the upper flange of the beam as the external vertical load increases from 0 kN to 200 kN. It is observed that using the TriPUR system reduces the strains in the bottom and the upper flanges of the beams more effectively than the other retrofit systems. This is because the CFRP plate has the largest eccentricity, e, compared to the other retrofit systems, which increases the moment of inertia of the beam cross-section at the mid-span.

It is clear from the results that the difference between the TPUR and the TriPUR systems is insignificant and that the performance of the retrofitted beams is mainly dependent on the CFRP pre-stress level rather than the type of the applied PUR system. Nevertheless, in some situations, for example, when there is no space to place the two deviators in the TPUR system, the TriPUR system, which only needs one deviator, can be used. Having said that, the TriPUR system needs a larger eccentricity between the CFRP plate and the beam. On the other hand, the FPUR or CPUR systems can be used

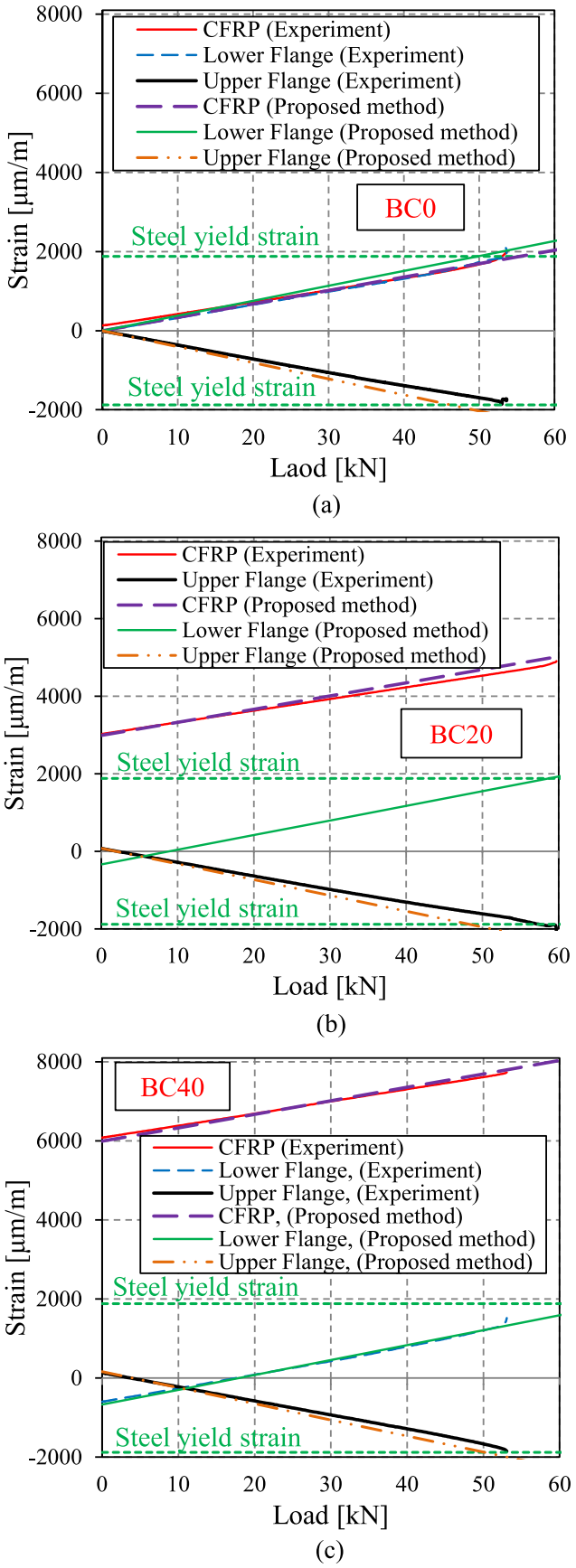

Fig. 15. The strain on the CFRP plate and the beam upper and lower flanges for Beam B strengthened by the CPUR system with (a) 0% (specimen BC0), (b) 20% (specimen BC20) and (c) 40% (specimen BC40) CFRP pre-stress level.

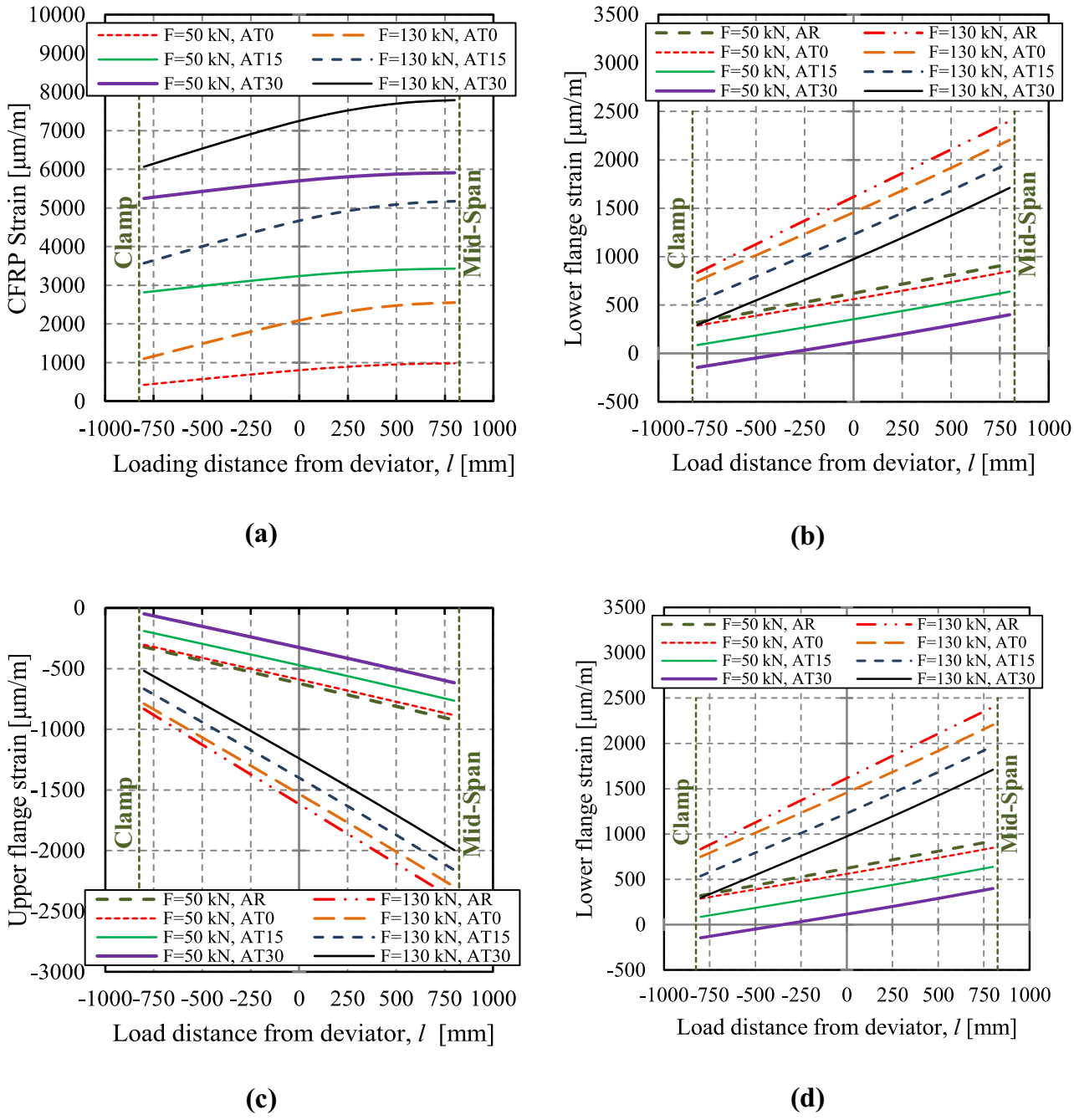

Fig. 16. The steel I-beams retrofitted by the TPUR system with different CFRP pre-stress levels of 0%, 15%, and 30% are subjected to vertical loads of 50 kN and 130 kN. The graphs show the strain on (a) the CFRP plate, (b) the beam's lower flange, (c) the beam's upper flange, and (d) the mid-span deflection in terms of position of the vertical load.

Table 4
Input parameters used in the proposed analytical model of the PUR systems (see Fig. 4).

System	e_C (mm)	a (mm)	b (mm)	L_e (mm)	l (mm)
TriPUR	55	825	1645	10	-820
FPUR	55	825	10	3280	+825
CPUR	1	825	825	1700	0

as alternatives when there is not enough room beneath the bridge (e.g., because of traffic) to apply the TPUR and the TriPUR systems. In general, from Figs. 17 and 18, all of the presented PUR systems result in similar improvements compared with the reference unstrengthened beams. Any of the presented PUR systems could be used for retrofitting of the metallic girders considering the ease of application, the available space beneath the bridge and the geometrical complexity of bridge elements.

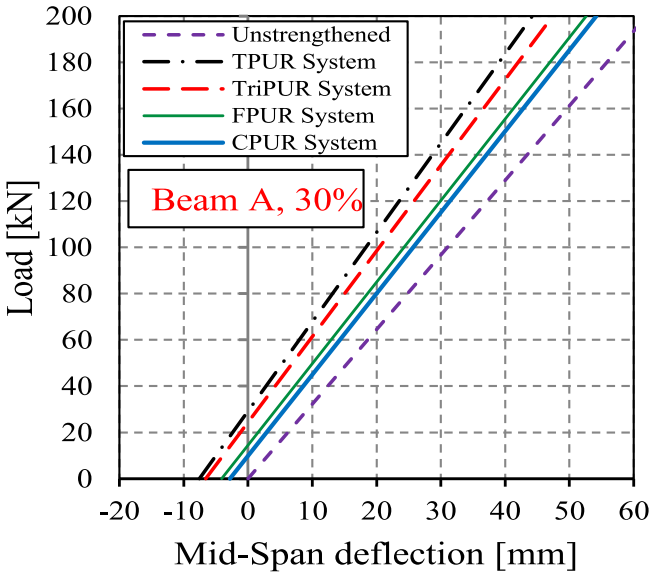

Fig. 17. The load–deflection behavior of the beams retrofitted by four different PUR systems, all with 30% CFRP pre-stress level.

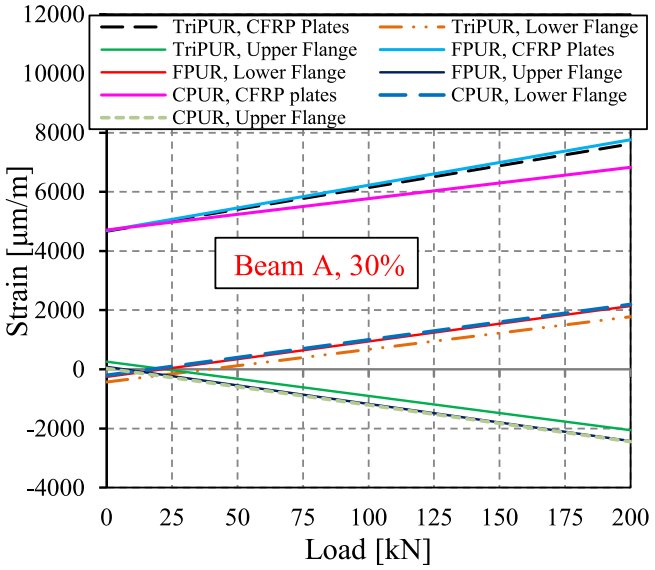

Fig. 18. The strains on the CFRP plates and the beam upper and lower flanges for the steel I-beams strengthened with four different PUR systems, all with 30% CFRP pre-stress level.

8. Conclusions

The concept of the un-bonded CFRP retrofit approach was explained. The un-bonded retrofit system can be used for strengthening of metallic members with rough (e.g., corroded) or obstructed (e.g., riveted or bolted) surfaces. The system offers a fast application procedure because there is no need for surface preparation prior to bond application. In this paper, four different variants of the PUR systems (i.e., the TPUR, TriPUR, FPUR and CPUR systems) were developed. The CFRP plates in the FPUR and the CPUR systems are very close to the beam bottom flange, and therefore, these two systems are appropriate for retrofitting girders where there is not much space beneath the bridge because of ongoing traffic.

A series of analytical solutions to predict the linear-elastic flexural behavior of the metallic beams retrofitted by the presented PUR systems was presented. The analytical method is based on the flexibility approach and can take into account the shear and the axial deformations in the beams. Furthermore, a detailed FE model was created to perform a numerical study on the behavior of the retrofitted metallic girders. The qualitative results of the developed analytical and numerical methods were compared with the results of the experiments on the aluminum and steel beams strengthened with the pre-stressed CFRP tendons and plates, respectively.

A series of parametric studies was performed to investigate the influence of the loading position, the CFRP pre-stress level and the distance between the supports and the clamps as well as the clamps and the deviators. The results showed that the efficiency of the retrofit method is mainly dependent on the CFRP pre-stress level rather than the type of the PUR system. Therefore, any variant of the PUR system that can ease application in the field can be considered for the retrofit solution.

Although strengthening using the PUR systems increases the stiffness of the beams, the magnitude of the CFRP pre-stress level does not make any contribution to the stiffness of the beams in the elastic domain. An increased CFRP pre-stress will decrease the deflections and increase the yield and ultimate load capacity of the beams. The results of this study showed that the pre-stressed un-bonded retrofit system could decrease the mid-span deflection of the beams about 30% and increase the yielding load capacity about 35% (compared with the reference unstrengthened specimen).

Appendix A. Deformations and strains in retrofitted beams

In this appendix, the mid-span deflection and the strain and the stress in different parts of the retrofitted beams (e.g., the upper flange, the lower flange and the CFRP plate) are calculated. The beam mid-span deflection, δ_M, is calculated as follows [31]:

$$\delta_M = \delta_{AB} + \delta_{BC} + \delta_{CM} + K(\delta_{AB}^{Shear} + \delta_{BC}^{Shear}) \tag{A.1}$$

where δ_i is the total vertical displacement at node i and

$$\delta_{AB} = \frac{F \cdot a^3}{3E_sI} + a\sin\theta_B \tag{A.2}$$

$$\delta_{BC} = \delta_{BC}^{F} - \delta_{BC}^{T} + b\sin\theta_C \tag{A.3}$$

δ_{BC}^{F} and δ_{BC}^{T} are the vertical displacements at node B relative to node C because of the external vertical force, F, and the tensile force of the CFRP plate, T, respectively

$$\delta_{BC}^{F} = \begin{cases} \frac{F(b^3+l^3)}{3E_sI} + \frac{(Fa)b^2}{2E_sI} - \frac{Fl^2(b+l)}{2E_sI} & -b < l < 0 \\ \frac{Fb^3}{3E_sI} + \frac{(Fa)b^2}{2E_sI} & 0 \leqslant l \leqslant \frac{L_e}{2} \end{cases} \tag{A.4}$$

$$\delta_{BC}^{T} = \frac{Tb^3\sin\varphi}{3E_sI} + \frac{Tb^2(e_c + \frac{h}{2})\cos\varphi}{2E_sI} \tag{A.5}$$

and

$$\delta_{CM} = \begin{cases} \frac{M_C L_e^2}{8E_sI} & -b < l < 0 \\ \frac{M_C L_e^2}{8E_sI} + \frac{Fl}{2E_sI}\left(\frac{L_e^2}{4} - \frac{l^2}{3}\right) + K\left(\frac{Fl}{G_sA_s}\right) & 0 \leqslant l \leqslant \frac{L_e}{2} \end{cases} \tag{A.6}$$

where G_s is the transverse shear modulus of the steel beam. The shear deformation is calculated as follows:

$$\delta_{AB}^{Shear} = \frac{Fa}{G_sA_s} \tag{A.7}$$

$$\delta_{BC}^{Shear} = \begin{cases} \frac{(F - T\sin\varphi)(b+l) + (T\sin\varphi)l}{A_sG_s} & -b < l < 0 \\ \frac{(F - T\sin\varphi)b}{A_sG_s} & 0 \leqslant l \leqslant \frac{L_e}{2} \end{cases} \tag{A.8}$$

The shear deformation of the steel beam is considered in the coefficient K. Coefficient K in Eq. (A.1) can be equal to zero or one. It is commonly neglected (e.g., for slender members) by setting K to zero.

In the above equations, δ_{ji} is the relative vertical displacement between nodes i and j

$$\delta_{ij} = \delta_j - \delta_i \tag{A.9}$$

In addition, the strain on the CFRP plate is given by

$$\varepsilon_P = \frac{\sigma_P}{E_P} = \frac{T}{E_P A_P} \tag{A.10}$$

The stress and the strain in the beam upper flange are

$$\sigma_b^u = \begin{cases} -\left(\frac{M_C h_0}{I} + \frac{T}{A_s}\right) & -b < l < 0 \\ -\left(\frac{M_C h_0}{I} + \frac{T}{A_s} + \frac{F l h_0}{I}\right) & 0 \leqslant l \leqslant \frac{L_e}{2} \end{cases} \tag{A.11}$$

and

$$\varepsilon_b^u = \frac{\sigma_b^u}{E_s} \tag{A.12}$$

The stress and the strain in the lower flange are

$$\sigma_b^l = \begin{cases} \frac{M_C h_0}{I} - \frac{T}{A_s} & -b < l < 0 \\ \frac{M_C h_0}{I} - \frac{T}{A_s} + \frac{F l h_0}{I} & 0 \leqslant l \leqslant \frac{L_e}{2} \end{cases} \tag{A.13}$$

and

$$\varepsilon_b^l = \frac{\sigma_b^l}{E_s} \tag{A.14}$$

References

[1] Yamada K, Ojio T, Inden T. Bridge monitoring and weigh-in-motion systems in Japan. Post-IABSE workshop on structural monitoring of bridges 2002.

[2] ASCE. Report Card for American Infrastructure, transportation Bridges. Grade C, American Society of Civil Engineering; 2009.

[3] Bień J, Elfgren L, Olofsson J, Edukacyjne DW. Sustainable bridges: assessment for future traffic demands and longer lives. Dolnośląskie Wydawnictwo Edukacyjne; 2007.

[4] IEAust. Report card on the nation's infrastructure. Australia: The Institution of Engineers; 1999.

[5] Ghafoori E. Fatigue strengthening of metallic members using un-bonded and bonded CFRP laminates (PhD dissertation). ETH-Zurich; 2015. http://dx.doi.org/10.3929/ethz-a-010453130.

[6] Ghafoori E, Motavalli M. A retrofit theory to prevent fatigue crack initiation in aging riveted bridges using carbon fiber-reinforced polymer materials. Polymers 2016;8(8):308.

[7] Deng J, Lee MM. Fatigue performance of metallic beam strengthened with a bonded CFRP plate. Compos Struct 2007;78(2):222–31.

[8] Zhao XL. FRP-strengthened metallic structures. Boca Raton, FL: Taylor and Francis; 2013.

[9] Ghafoori E. Interfacial stresses in beams strengthened with bonded prestressed plates. Eng Struct 2013;46:508–10.

[10] Ghafoori E, Motavalli M. Flexural and interfacial behavior of metallic beams strengthened by prestressed bonded plates. Compos Struct 2013;101:22–34.

[11] IA 263:2003 steel structures. Zürich: Schweizerische Normen-Vereinigung; 2003.

[12] Colombi P, Fava G. Experimental study on the fatigue behaviour of cracked steel beams repaired with CFRP plates. Eng Fract Mech 2015;145:128–42.

[13] Colombi P, Fava G. Fatigue crack growth in steel beams strengthened by CFRP strips. Theoret Appl Fract Mech 2016.

[14] Colombi P, Fava G, Sonzogni L. Fatigue behavior of cracked steel beams reinforced by using CFRP materials. Proc Eng 2014.

[15] Colombi P, Fava G, Sonzogni L. Fatigue crack growth in CFRP-strengthened steel plates. Compos B Eng 2015;72:87–96.

[16] Dawood M, Rizkalla S, Sumner E. Fatigue and overloading behavior of steel-concrete composite flexural members strengthened with high modulus CFRP materials. J Compos Constrt 2007;11(6):659–69.

[17] Wu C, Zhao XL, Al-Mahaidi R, Emdad M, Duan W. Fatigue tests of cracked steel plates strengthened with UHM CFRP plates. Adv Struct Eng 2012;15(10):1801–16.

[18] Wu C, Zhao XL, Chiu WK, Al-Mahaidi R, Duan WH. Effect of fatigue loading on the bond behaviour between UHM CFRP plates and steel plates. Compos B Eng 2013;50:344–53.

[19] Ghafoori E, Motavalli M, Nussbaumer A, Herwig A, Prinz G, Fontana M. Determination of minimum CFRP pre-stress levels for fatigue crack prevention in retrofitted metallic beams. Eng Struct 2015;84:29–41.

[20] Ghafoori E, Motavalli M, Zhao XL, Nussbaumer A, Fontana M. Fatigue design criteria for strengthening metallic beams with bonded CFRP plates. Eng Struct 2015;101:542–57.

[21] Ghafoori E, Motavalli M. Analytical calculation of stress intensity factor of cracked steel I-beams with experimental analysis and 3D digital image correlation measurements. Eng Fract Mech 2011;78(18):3226–42.

[22] Ghafoori E, Schumacher A, Motavalli M. Fatigue behavior of notched steel beams reinforced with bonded CFRP plates: determination of prestressing level for crack arrest. Eng Struct 2012;45:270–83.

[23] Al-Zubaidy H, Al-Mahaidi R, Zhao XL. Experimental investigation of bond characteristics between CFRP fabrics and steel plate joints under impact tensile loads. Compos Struct 2012;94(2):510–8.

[24] Dawood M, Rizkalla S. Environmental durability of a CFRP system for strengthening steel structures. Constr Build Mater 2010;24(9):1682–9.

[25] Ghafoori E, Motavalli M. Lateral-torsional buckling of steel I-beams retrofitted by bonded and un-bonded CFRP laminates with different pre-stress levels: experimental and numerical study. Constr Build Mater 2015;76:194–206.

[26] Ghafoori E, Motavalli M. Normal, high and ultra-high modulus CFRP laminates for bonded and un-bonded strengthening of steel beams. Mater Des 2015;67:232–43.

[27] Ghafoori E, Motavalli M. Innovative CFRP-prestressing system for strengthening metallic structures. J Compos Constr 2015;19(6):04015006.

[28] Ghafoori E, Motavalli M, Nussbaumer A, Herwig A, Prinz GS, Fontana M. Design criterion for fatigue strengthening of riveted beams in a 120-year-old railway metallic bridge using pre-stressed CFRP plates. Compos B Eng 2015;68:1–13.

[29] Timoshenko SP, Young DH. Theory of structures, vol. 15. New York: McGraw-Hill; 1965.

[30] Boresi AP, Schmidt RJ, Sidebottom OM. Advanced mechanics of materials, vol. 5. New York: Wiley; 1993.

[31] Hibbeler RC. Structural analysis. 8th ed. Upper Saddle River, NJ 07458: Pearson Education Inc.; 2014.

[32] Zhu P, Fan H, Zhou Y. Flexural behavior of aluminum I-beams strengthened by pre-stressed CFRP tendons. Constr Build Mater 2016;122:607–18.